

# Optimal Energy Management Strategy including Battery Health through Thermal Management for Hybrid Vehicles

Thomas MIRO PADOVANI\* Maxime DEBERT\*  
Guillaume COLIN\*\* Yann CHAMAILLARD\*\*

\* Renault SAS, France, (e-mail: {Thomas.Miro-Padovani,  
maxime.debert}@renault.com)

\*\* Laboratoire PRISME, Université d'Orléans, France, (e-mail:  
{guillaume.colin, yann.chamaillard}@univ-orleans.fr)

---

**Abstract:** The paper proposes an energy management strategy (EMS) for hybrid electric vehicles (HEV) and plug-in hybrid electric vehicles (PHEV) taking into account battery health through an additional soft constraint on battery internal temperature, considered as one of the prime factors influencing battery aging. Battery cell temperature is modeled and considered as a second state constraint with the state of energy (SOE) in the optimization problem solved on-line using the equivalent consumption minimization strategy (ECMS). Simulation results are presented to highlight the contribution of the strategy including battery thermal management compared to the standard approach.

*Keywords:* Energy management strategy, Plug-in hybrid electric vehicles, Li-ion battery aging, thermal management, Pontryagin's Minimum Principle.

---

## 1. INTRODUCTION

The interest for energy management strategy (EMS) of Hybrid electric vehicles has been growing over the past decade, Guzzella and Sciarretta (2007). It is commonly acknowledged that supervisory control of HEV and PHEV plays a critical part in the global performance of these vehicles. Optimal control theory is often relied upon to achieve this difficult task, off line (Dynamic Programming (DP) Sunström et al. (2008), Pontryagin's Minimum Principle (PMP) Sciarretta et al. (2004)) as well as on line (Equivalent Consumption Minimization Strategy (ECMS) Chasse et al. (2010), Stochastic Dynamic Programming (SDP) Moura et al. (2009)). Traditionally, the cost function to minimize is the fuel consumption (equivalent to  $CO_2$  emissions) over a given trip.

The battery is often considered as the centerpiece of a hybrid electric application, especially for PHEV, mainly because of its substantial cost and the fact that its performances fade over time. Matching the battery and vehicle lifetimes is a crucial issue to improve the economic viability of HEV. Again, the stake is even higher for PHEV which rely significantly more on electric energy. If used properly, the degree(s) of freedom offered by hybrid powertrains can contribute to slowing down aging mechanisms by avoiding as much as possible operating conditions harmful to the battery. The contribution of the paper is to propose a battery friendly energy management strategy by adding an aging related cost to the criterion to be minimized. While several authors have submitted interesting ideas to take into account battery health in the EMS, Serrao et al. (2011), Ebbesen et al. (2012), the issue remains to be dealt with.

Battery aging is irreversible and results in two main factors: capacity fading and increasing internal resistance. The first phenomenon tends to lessen storable energy, and therefore reduces the electric range of the vehicle. The second lowers maximum available power and battery overall efficiency. Battery aging is monitored by the on-board battery management system (BMS) and is commonly expressed as a non-dimensional parameter, the state of health (SOH) Remmlinger et al. (2011), decreasing from 1 (brand new) to 0 (worn out) as the battery wears. The aging process of Li-ion batteries is very intricate and is currently the subject of many studies, Gyan et al. (2011). Aging mechanisms will differ between the anode and cathode, also depending on the material and structural features of the cell. Furthermore, most of these processes are interdependent. Readers interested in a thorough analysis on Li-ion battery aging can refer to Vetter et al. (2005), Broussely et al. (2005).

The primary factors enhancing battery aging are high temperatures and high states of charge. As a consequence, the strategy presented in this paper includes a penalty regarding undesired battery temperatures in the optimality criterion. The objective is to combine energy and thermal management and thus ensure a trade-off between powertrain efficiency and battery aging via a soft constraint on cell temperature. While suboptimal, the proposed strategy is on-line oriented and does not require the tuning of an extra co-state. Therefore the complexity of the solution remains equivalent to a standard ECMS. The case studied in the paper is based on a Li-ion battery, more suitable for PHEV. However, the methodology remains valid and relevant for any technology, since high temperature is always a factor contributing to battery aging, regardless

of its type.

The considered battery model has been designed so as to be consistent with the information available from an actual battery pack. It describes the dynamics of both the cell temperature and the state of energy (SOE) Mamadou et al. (2010), more suitable for PHEV than the classical state of charge (SOC). The battery model is presented in Section 2. The optimization problem with the additional battery temperature constraint is formulated in Section 3 and solved using Pontryagin's Minimum Principle. The on-line counterpart of the PMP, known as equivalent consumption minimization strategy is implemented and the simulation results yielded are presented and discussed in Section 4.

## 2. BATTERY MODEL

### 2.1 Internal temperature

So as to implement a battery thermal management strategy, a control-oriented model of the battery cells' temperature has to be designed. The zero-dimensional model considered is based on the heat transfer equations between a cell and the air surrounding the battery pack Muratori et al. (2010). The main assumption is a homogeneous temperature of the cells. A depiction of the model's heat transfers is given in Fig. 1. The prismatic cells are enclosed in modules composing the battery pack. As a result, four temperatures are considered:  $T_{cell}$  is the cell temperature,  $T_{sens}$  is the temperature of the air confined in the module which is given by a sensor on an actual battery pack,  $T_{cas}$  is the temperature of the module casing and finally  $T_{air}$  is the air temperature around the battery pack. The temperature model presented in Lin et al. (2013) is based on a similar approach but applied to cylindrical cells and using an observer to consolidate the estimation. The battery thermal model can be written as a state space model:

$$\dot{T}_{cell} = k_1 (RI_{bat}^2 - k_4(T_{cell} - T_{sens})) \quad (1)$$

$$\dot{T}_{sens} = k_2 (k_4(T_{cell} - T_{sens}) - k_5(T_{sens} - T_{cas})) \quad (2)$$

$$\dot{T}_{cas} = k_3 (k_5(T_{sens} - T_{cas}) - k_6(T_{cas} - T_{air})), \quad (3)$$

with the parameters:

$$\begin{cases} k_1 = \frac{1}{C_{v1}}, & k_2 = \frac{1}{C_{v2}}, & k_3 = \frac{1}{C_{p3}}, \\ k_4 = \frac{1}{R_{eq1}}, & k_5 = \frac{1}{R_{eq2}}, & k_6 = \frac{1}{R_{eq3}}. \end{cases} \quad (4)$$

The cell's internal resistance  $R$  is given here by a look-up table, as a function of the state of charge (SOC) and cell temperature  $T_{cell}$ :

$$R = f(SOC, T_{cell}). \quad (5)$$

The battery current  $I_{bat}$  is available on-board, measured by the battery management system. The equivalent thermal resistances  $R_{eqi}$  (K/W) correspond respectively to the surface of the cell, sensor, and casing. The heat capacities (J/K)  $C_{v1}$ ,  $C_{v2}$ , and  $C_{p3}$  refer to the cell, the air enclosed in the module, and the module casing. These parameters have been identified using data provided by an experiment on a battery module mounted with specific thermal sensors. Fig. 2 shows a comparison between the thermal model

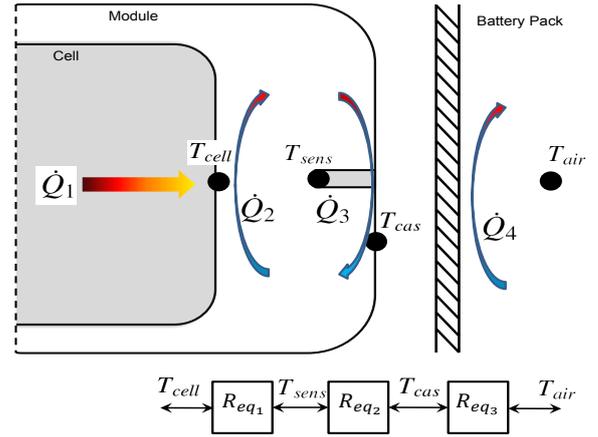


Fig. 1. Heat flow transfers with equivalent resistance modeling

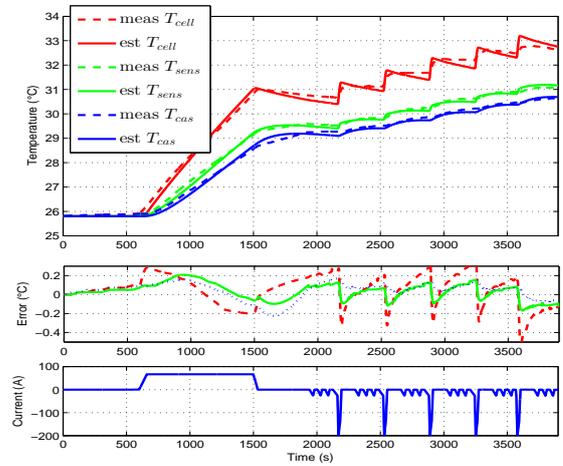


Fig. 2. Thermal model identification

values and experimental data. The model as well as the validation process are explained in more detail in Debert et al. (2013). Considering the sensor temperature in the model is relevant for an on-line application where the sensor temperature given by the actual battery pack allows the implementation of a cell temperature observer, enhancing the performances of the resulting closed-loop model Debert et al. (2013). The cell temperature observer is essential to ensure both a faithful estimation and robustness with cell dispersion for on-board applications but is not used with the battery model presented in this paper.

### 2.2 State of energy

In order for the energy management strategy to be consistent with PHEV operations the state of energy approach is favored over the classical state of charge calculation Stockar et al. (2011). While the SOC is a fair representation of the energy remaining in the battery when considering charge sustaining operation, it is no longer the case for high depletion conditions. For HEV, the SOC is sustained around 50%, where the open circuit voltage (OCV) of the battery is almost constant, therefore battery current and power flow can be considered proportional. As for a PHEV, the OCV decreases significantly with charge depletion,

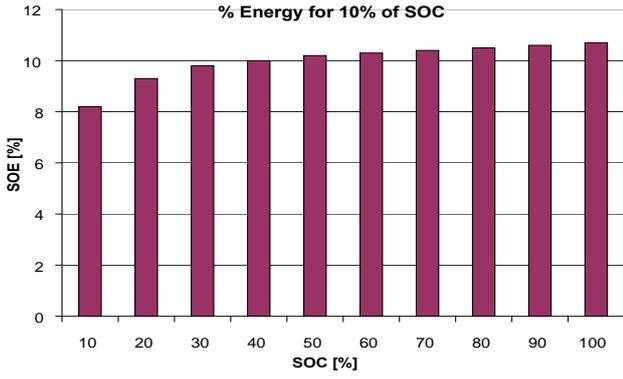


Fig. 3. SOE contained in each tenth of battery SOC

consequently current cannot be considered a faithful image of power flow. Ultimately the charge remaining in the battery is not an accurate estimation of the energy left, which is an important piece of information to assess the electric range of a PHEV. Fig. 3 shows the amount of energy contained in each tenth of state of charge for a Li-ion battery. The percentage of energy in each tenth decreases as does the state of charge and therefore the OCV. The main consequence is that considering the same driving pattern, the vehicle will travel further depleting the battery SOC from 100% to 90% than from 10% to 0%. The SOE is defined by:

$$\zeta(P_{bat}, SOC) = \frac{E_R(P_{bat}, SOC)}{E_N} \quad (6)$$

$$= \frac{E_{t_0} - \int_{t_0}^t OCV(SOC) \cdot I_{bat}(P_{bat}, SOC) dt}{E_N},$$

with  $I_{bat}$  the battery current, often modeled by:

$$I_{bat} = \frac{OCV(SOC) + \sqrt{OCV^2(SOC) - 4P_{bat} \cdot R}}{2 \cdot R}, \quad (7)$$

Guzzella and Sciarretta (2007) and where  $E_R$  is the energy remaining in the battery,  $P_{bat}$  the reversible electric power exchanged with the battery, and  $E_N$  its nominal energy capacity (when fully charged):

$$E_N = OCV_{Max} \cdot Q_{Max}. \quad (8)$$

The SOE dynamics can be written:

$$\begin{aligned} \dot{\zeta}(P_{bat}, SOC) &= -\frac{OCV(SOC) \cdot I_{bat}(P_{bat}, SOC)}{E_N} \\ &= -\frac{I_{bat}(P_{bat}, SOC)}{Q_{Max}} \cdot \frac{OCV(SOC)}{OCV_{max}} \\ &= \dot{SOC}(P_{bat}, SOC) \cdot \frac{OCV(SOC)}{OCV_{Max}}. \end{aligned} \quad (9)$$

Equation (9) highlights the fact that when considering charge sustaining operation  $OCV(SOC)$  can be assumed constant, therefore the dynamics of the SOC and SOE are identical. However, this is not the case for charge depleting conditions where  $OCV(SOC)$  induces a non-linearity between the two dynamics. Fig. 3 also illustrates this phenomenon, showing the near equivalence between SOC and SOE at 50% SOC but not at low or high SOC.

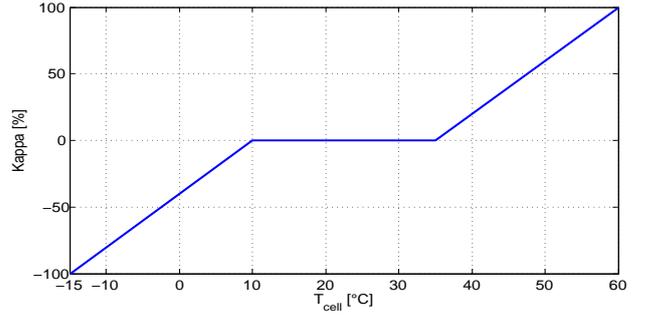


Fig. 4. Weighting factor  $\kappa$  versus cell temperature

### 3. ENERGY MANAGEMENT STRATEGY

The energy management strategy, based on optimal control theory, seeks to minimize a global criterion over the total length of the trip. The criterion is defined by a cost function, most commonly the fuel consumption only. It is however possible to consider a more global cost function made of several costs in order to implement additional constraints, for example on drivability Debert et al. (2012), pollutant emissions Michel et al. (2012), or powertrain temperatures Lescot et al. (2010). In this paper, the proposed cost function includes an additional cost on battery temperature evolution in addition to the fuel consumption:

$$J = \int_{t_1}^{t_2} \dot{m}_f(u(t), T_{wheel}(t)) + \kappa(T_{cell}) \dot{T}_{cell}(u(t), T_{cell}) dt + \Phi(\zeta(t_2)) + \Psi(T_{cell}(t_2)), \quad (10)$$

with

$$\Phi(\zeta(t_2)) = \begin{cases} 0 & \text{if } \zeta(t_2) \geq SOE_{final} \\ \infty & \text{else,} \end{cases} \quad (11)$$

$$\Psi(T_{cell}(t_2)) = 0.$$

Where  $\dot{m}_f$  is the instantaneous fuel consumption,  $u$  is the control variable,  $T_{wheel}$  is wheel torque request, imposed by the driver or a driving cycle (speed profile).  $\dot{T}_{cell}$  is the cell temperature fluctuation and  $\kappa$  is a weighting parameter depending on the cell temperature, as represented in Fig. 4. The chosen control variable  $u = P_{bat}$ , is the power delivered by the battery, which has to be optimized by the EMS to minimize the criterion  $J$ .  $\Phi(\zeta(t_2))$  is a function ensuring a solution meeting the final requirement on the SOE. The final SOE will be chosen equal to its initial value for sustaining operation, but will be close to the minimal SOE admissible by the battery for depleting operation. The function  $\Psi(T_{cell}(t_2))$  is set to 0 since no constraint is considered for the cell's final temperature. The above system has 2 state variables:

$$\mathbf{x} = \left\{ \begin{array}{c} \zeta \\ T_{cell} \end{array} \right\},$$

the SOE and battery cell temperature. Their dynamics have been defined in Section 2 with respectively (9) and (1).

The key idea behind this additional cost is to penalize the commands causing the battery temperature to get further away from its slow-aging operating range, and to favor the ones that get the temperature closer. The weighting factor

$\kappa$  will allow a trade-off between fuel consumption and safe battery temperature. Set to 0 when the battery operates in its slow-aging zone, there will be no additional cost and only fuel consumption will be minimized. On the other hand,  $\kappa$  increases when the temperature gets past the slow-aging zone, the higher the temperature the higher the cost, to prevent the temperature from rising further. On the opposite, the negative cost caused by negative values of  $\kappa$  when the temperature is too cold favors battery warming, once again to get it closer to the slow-aging zone. To minimize the global criterion (10), the Pontryagin's Minimum Principle states that the optimal control  $u_{opt}(t)$  has to minimize, for all  $t \in [t_1, t_2]$ , the following Hamiltonian function:

$$H(u, \mathbf{x}, T_{wheel}, \lambda_\zeta, \lambda_{T_{cell}}) = \dot{m}_f(u, T_{wheel}) + \kappa(T_{cell})\dot{T}_{cell}(u) + \lambda_\zeta(t)\dot{\zeta}(u) + \lambda_{T_{cell}}(t)\dot{T}_{cell}(u), \quad (12)$$

and

$$u_{opt}(t) = \underset{P_{bat}}{\operatorname{argmin}} H(u, \mathbf{x}, T_{wheel}, \lambda_\zeta, \lambda_{T_{cell}}). \quad (13)$$

Where  $\lambda_\zeta(t)$  is the SOE co-state defined by the Euler-Lagrange equation:

$$\dot{\lambda}_\zeta(t) = -\frac{\partial H}{\partial \zeta} = -\lambda_\zeta(t) \frac{\partial \dot{\zeta}(u)}{\partial \zeta} \simeq 0, \quad (14)$$

this co-state is commonly considered constant since  $\frac{\partial \dot{\zeta}(P_{bat}, SOC)}{\partial \zeta} \simeq 0$  for a large range of SOE Stockar et al. (2011), thus:

$$\lambda_\zeta(t) = \lambda_\zeta. \quad (15)$$

The dynamics of second co-state on cell temperature is defined as:

$$\begin{aligned} \dot{\lambda}_{T_{cell}}(t) &= -\frac{\partial H}{\partial T_{cell}} \\ &= -\frac{\partial(\kappa(T_{cell})\dot{T}_{cell}(u))}{\partial T_{cell}} - \lambda_{T_{cell}}(t) \frac{\partial \dot{T}_{cell}(u)}{\partial T_{cell}} \end{aligned} \quad (16)$$

The partial derivative of (1) with respect to  $T_{cell}$  gives:

$$\frac{\partial \dot{T}_{cell}}{\partial T_{cell}} = -k_1 k_4. \quad (17)$$

Therefore:

$$\dot{\lambda}_{T_{cell}}(t) = -\frac{\partial \kappa(T_{cell})}{\partial T_{cell}} \dot{T}_{cell}(u) + k_1 k_4 (\lambda_{T_{cell}}(t) + \kappa(T_{cell})). \quad (18)$$

In the identified model  $k_1 k_4$  is about  $10^{-3}$ , as a consequence the assumption  $k_1 k_4 \simeq 0$  is made. The cell temperature dynamic is very slow,  $|\dot{T}_{cell}| \leq 3.10^{-3} \simeq 0$

and  $\kappa(T_{cell})$  as chosen Fig. (4) gives  $\left| \frac{\partial \kappa(T_{cell})}{\partial T_{cell}} \right| < 15$

and  $\frac{\partial \kappa(T_{cell})}{\partial T_{cell}} = 0$  in the slow-aging zone. As a result, we suppose:

$$\dot{\lambda}_{T_{cell}}(t) \simeq 0. \quad (19)$$

Vehicle mass	1400 kg
Engine maximum power	85 kW
Electric motor maximum power	40 kW
Battery energy capacity	7 kWh

Table 1. Vehicle characteristics

The lack of constraint on the final cell temperature, giving  $\Psi(T_{cell}(t_2)) = 0$ , leads to

$$\lambda_{T_{cell}}(t_2) = 0. \quad (20)$$

Finally (19) and (20) imply:

$$\lambda_{T_{cell}} = 0 \quad (21)$$

The Hamiltonian function (12) is ultimately simplified to:

$$H(u, \mathbf{x}, T_{wheel}, \lambda_\zeta) = \dot{m}_f(u, T_{wheel}) + \lambda_\zeta \dot{\zeta}(u) + \kappa(T_{cell}) \dot{T}_{cell}(u). \quad (22)$$

In practice, the command  $P_{bat}$  is discretized between the minimum and maximum battery power tolerated by the powertrain, and the value minimizing (22) is chosen as the optimal command  $u_{opt}(t)$ . The process must be repeated for each time step of the simulation.

#### 4. SIMULATION RESULTS

Simulation results are based on a quasi-static model of the vehicle and powertrain. The vehicle's dynamics is given by Newton's second law. As for the hybrid powertrain, engine, electrical machine and battery efficiencies are computed using look up tables. The PHEV considered is provided with a parallel hybrid powertrain, its main characteristics are given in table 1. The results presented were obtained considering an on-line optimization of  $\lambda_\zeta$ . It means that a unique value of  $\lambda_\zeta(t_1)$  is chosen, remaining the same for each simulation. The co-state is then adjusted on-line during simulation by a proportional-integral controller in order to regulate the SOE to the desired value. This approach does not yield strictly optimal results, but is more representative of what could be implemented in an actual vehicle. The following results are based on four scenarios, considering different operating conditions and external temperature. For each simulation, the initial battery temperature is set to the external temperature.

The first scenario discussed is based on nominal conditions and charge sustaining operation. The ambient temperature is set to 15°C. The trip considered is made of a succession of the Artemis road and Artemis urban cycles, the total length of the trip is 58 km. Fig. 5 shows the evolution of the cell temperature with the thermal constraint, together with the chosen speed profile. One can notice that in these conditions the cell temperature remains in the slow-aging zone, here set between 10 and 35°C. Therefore the weighting factor  $\kappa$  stays equal to 0 during the whole trip. This means that the thermal constraint remains idle, the optimization problem is identical to the regular fuel-consumption-only criterion. In the end, no extra fuel consumption is introduced.

For the second scenario, charge sustaining operation in cold weather is considered, the external air temperature is set to 0°C. The driving cycle is the same as for the first scenario. Fig. 6 displays the cell temperature along the trip with and without battery thermal management. The

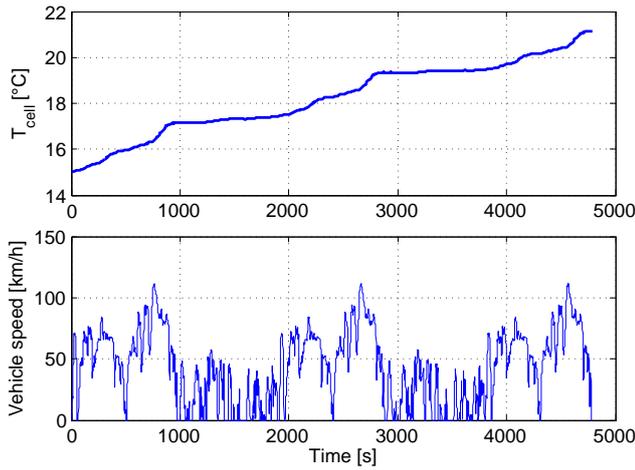


Fig. 5. Cell temperature evolution during nominal operating conditions and followed driving cycle

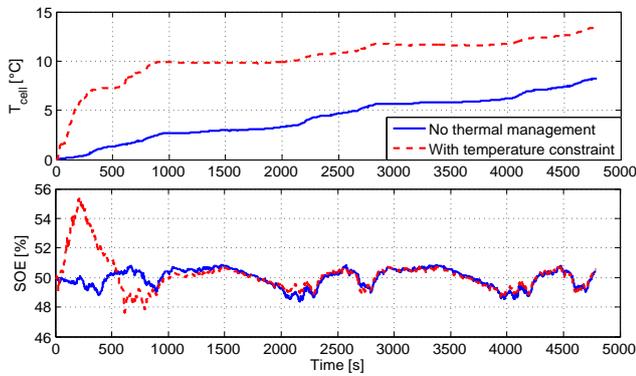


Fig. 6. Cell temperature and battery SOE with and without thermal management during cold operation

temperature penalty favors the battery warm-up by over-relying on electric energy until the temperature reaches the slow-aging zone (around 1000s). Subsequently  $\kappa$  remains equal to 0, as a result the temperature constraint is idle for the rest of the trip. The second part of Fig. 6 shows the SOE evolution, with battery thermal management the engine is relied upon to charge the battery at the beginning of the trip, causing the cell temperature to rise. The extra electric energy gathered is then depleted to meet the charge sustaining requirement. One may notice that the SOE remains very close to 50% during the entire cycle, this is due to the high energetic capacity of the battery (7kWh) designed for PHEV applications. However, since cell resistance is higher at low temperature, it is important to ensure that battery current does not get too high, so as to stay in the acceptable voltage range of the cells. This requirement is commonly taken care of by the battery management system. As expected, warming up the battery leads to extra fuel consumption in order to compensate the energy dissipated on purpose. For this specific scenario the extra fuel consumption reaches 3%. Yet it is worth noting that the relative extra consumption will strongly depend on the total fuel required to complete the trip.

The third scenario assumes charge sustaining operation and 30°C for the external temperature. The trip considered is made of twice previous trip presented in a row, thus 116 km total. For this specific scenario, the slow-

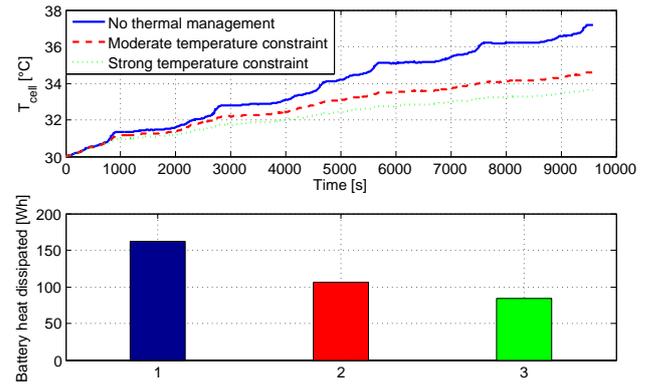


Fig. 7. Cell temperature and total heat released for 3 levels of temperature constraint

aging zone is set between 10 and 30°C. Fig. 7 shows the cell temperature for 3 cases: no temperature constraint, moderate, and strong temperature constraint. This illustrates the fact that by tuning the parameter  $\kappa$ , one is able to modulate the trade-off between fuel consumption and battery thermal constraint. For this simulation, the extra fuel consumption lead by the thermal management is 0.7% and 1.1% respectively for the moderate and strong constraint. As for the cell temperature, it is reduced by respectively 2.6 and 3.6°C at the end of the trip. The lowest part of Fig. 7 shows the total heat released by the battery (Wh) during the whole trip for the 3 constraints. As expected, the stronger the constraint the lower the heat dissipated, which explains how the strategy reduces battery warming.

Finally, the fourth scenario considers a plug-in hybrid taxi alternating between quick charges and the trip presented in Fig. 5 for almost 7 hours. The external temperature is set to 25°C. The charging power is at first set to 35 kW and then decreases in order for the battery to remain in its admissible voltage range. When the charge is completed, the battery has a resting period of 10 minutes. The trip is carried out in charge depleting charge sustaining (CDCS) mode. It means that the first part of the trip is done using electrical energy as much as possible, close to an electric vehicle. Once the battery is depleted the vehicle enters charge sustaining mode until the next charge. Fig. 8 shows the difference between cell temperature with and without battery thermal management. The temperature constraint manages to reduce the cell temperature of several degrees, there is ultimately a 3°C difference at the end of the day. Although the difference may seem thin, the gain on battery life lies on the long term, if repeated on a daily basis. Moreover, as presented in Fig. 8, the temperature reduction is obtained by avoiding high currents, also one of the main factors contributing to battery aging. Since the heat production of the cells is given by  $P_{heat} = RI_{bat}^2$ , the EMS avoids currents above 70 A to moderate the temperature increase. Therefore, the temperature management is beneficial in two ways: lower temperature and lower current. The extra fuel consumption introduced by the thermal management is 1.4% for this scenario.

The simulation results presented above illustrate the fact that the proposed strategy manages to restrain, or on the opposite favor battery warming. However, during common operating conditions the temperature constraint will be

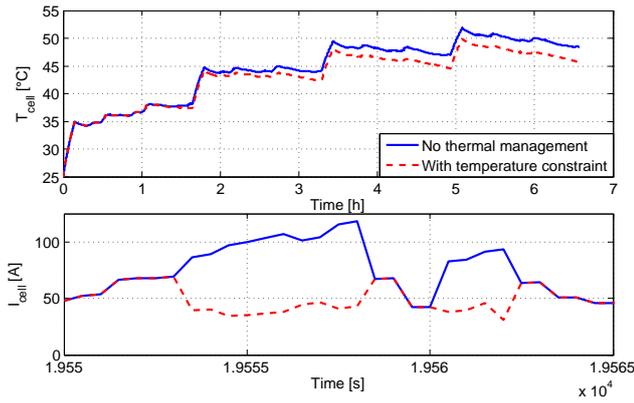


Fig. 8. Cell temperature (up) and zoom on battery current (down) with and without thermal management during severe operating conditions

idle, allowing the minimization of fuel consumption only. It is worth noting that the strategy avoids high currents in order to reduce battery warming, which is also profitable to limit battery aging. The trade-off between fuel consumption and temperature constraint as well as the desired battery temperature operating range are set by tuning one parameter:  $\kappa(T_{cell})$ . Moreover, the strategy is relevant for both HEV and PHEV. Finally, results tend to show that the effect of battery temperature constraint on fuel consumption remains moderate.

## 5. CONCLUSION

Battery temperature is known to be one of the main factors contributing to battery aging, whatever the technology. Therefore the EMS proposed in this paper considers a soft constraint on battery temperature, as an additional cost in the criterion to be minimized. The problem is solved using Pontryagin's Minimum Principle, with a suboptimal but on-line-oriented solution. The loss of optimality is compensated by the fact that the proposed strategy requires no extra co-state and is therefore easily applicable to a standard optimal on-line EMS. The resulting EMS combines powertrain efficiency and battery thermal management, allowing for both an optimized fuel consumption and battery health preservation. The strategy applies to both HEV and PHEV, but might be more relevant for vehicles provided with light or non-existent battery thermal regulation. Simulation results highlight the potential of the strategy for different scenarios, but also the fact that the temperature constraint remains idle during more lenient operations. A weighting factor allows to choose the temperature range where the constraint will remain idle, as well as the constraint's intensity when the battery temperature is out of bound. It is however very difficult to express the actual amount of Ah-throughput, that is battery lifetime, saved by the strategy. It will indeed depend on numerous factors: battery technology, operating conditions (external temperature, current profile, SOC range), for battery aging is a very complex phenomenon.

## REFERENCES

Broussely, M., Biensan, P., Bonhomme, F., Blanchard, P., Herreyre, S., Nechev, K., and Staniewicz, R. (2005). Main aging mechanisms in Li ion batteries. *Journal of Power Sources*, 146(1-2), 90–96.

- Chasse, A., Sciarretta, A., and Chauvin, J. (2010). Online optimal control of a parallel hybrid with costate adaptation rule. In *Proceedings of the 2010 IFAC Symposium Advances in Automotive Control*.
- Debert, M., Colin, G., Bloch, G., and Chamaillard, Y. (2013). An observer looks at the cell temperature in automotive battery packs. *Control Engineering Practice*, 21(8), 1035–1042.
- Debert, M., Miro-Padovani, T., Colin, G., Chamaillard, Y., and Guzzella, L. (2012). Implementation of comfort constraints in dynamic programming for hybrid vehicle energy management. *International Journal of Vehicle Design*, 58(2-3-4), 367–386.
- Ebbesen, S., Elbert, P., and Guzzella, L. (2012). Battery state-of-health perceptive energy management for hybrid electric vehicles. *IEEE Transactions on Vehicular Technology*, 61, 2893–2900.
- Guzzella, L. and Sciarretta, A. (2007). *Vehicle Propulsion Systems. Introduction to Modeling and Optimization*. Springer, 2 edition.
- Gyan, P., Aubret, P., Hafsaoui, J., Sellier, F., Bourlot, S., Zinola, S., and Badin, F. (2011). Experimental assessment of battery cycle life within the simstock research program. In *Proceedings of the 2011 Les Rencontres Scientifiques d'IFP Energies Nouvelles*.
- Lescot, J., Sciarretta, A., Chamaillard, Y., and Charlet, A. (2010). On the integration of optimal energy management and thermal management of hybrid electric vehicles. In *Proceedings of the 2010 IEEE Vehicle Power and Propulsion Conference*.
- Lin, X., Perez, H.E., Siegel, J.B., Stefanopoulou, A.G., Li, Y., Anderson, R.D., Ding, Y., and Castanier, M.P. (2013). On-line parameterization of lumped thermal dynamics in cylindrical lithium ion batteries for core temperature estimation and health monitoring. *IEEE Transactions on Control System Technology*, Accepted pending minor revisions.
- Mamadou, K., Delaille, A., Lemaire-Potteau, E., and Bultel, Y. (2010). The state-of-energy: A new criterion for the energetic performances evaluation of electrochemical storage devices. *The Electrochemical Society Transactions*, 25, 105–112.
- Michel, P., Charlet, A., Colin, G., Chamaillard, Y., Nouillant, C., and Bloch, G. (2012). Energy management of hev to optimize fuel consumption and pollutant emissions. In *Proceedings of the 2012 International Symposium on Advanced Vehicle Control*.
- Moura, S.J., Fathy, H.K., Callaway, D.S., and Stein, J.L. (2009). A stochastic optimal control approach for power management in plug-in hybrid electric vehicles. *IEEE Transactions on control systems technology*, 19, 545–555.
- Muratori, M., Canova, M., Guezennec, Y., and Rizzoni, G. (2010). A reduced-order model for the thermal dynamics of Li-Ion battery cells. In A. Trächtler and D. Abel (eds.), *Proceedings of the 6th IFAC Symposium Advances in Automotive Control*. Munich, Germany.
- Remmlinger, J., Buchholz, M., Meiller, M., Bernreuter, P., and Dietmayer, K. (2011). State-of-health monitoring of lithium-ion batteries in electric vehicles by on-board internal resistance estimation. *Journal of Power Sources*, 196, 5357–5363.
- Sciarretta, A., Back, M., and Guzzella, L. (2004). Optimal control of parallel hybrid electric vehicles. *IEEE Transactions on control systems technology*, 12, 352–363.
- Serrao, L., Onori, S., Sciarretta, A., Guezennec, Y., and Rizzoni, G. (2011). Optimal energy management of hybrid electric vehicles including battery aging. In *Proceedings of the 2011 American Control Conference*.
- Stockar, S., Marano, V., Canova, M., Rizzoni, G., and Guzzella, L. (2011). Energy-optimal control of plug-in hybrid electric vehicles for real-world driving cycles. *IEEE Transactions on Vehicular Technology*, 60(7), 2949–2962.
- Sunström, O., Guzzella, L., and Soltic, P. (2008). Optimal hybridization in two parallel hybrid electric vehicles using dynamic programming. In *Proceedings of 17th World Congress The International Federation of Automatic Control Seoul*. Korea.
- Vetter, J., Novak, P., Wagner, M., Veit, C., Möller, K.C., Besenhard, J., Winter, M., Wohlfart-Mehrens, M., Vogler, C., and Hammouche, A. (2005). Ageing mechanisms in lithium-ion batteries. *Journal of Power Sources*, 147(1-2), 269–281.